# International Competition on
# **Cells Classification by Fluorescent Image Analysis**

hosted by the
20th International Conference on Image Processing (ICIP 2013)

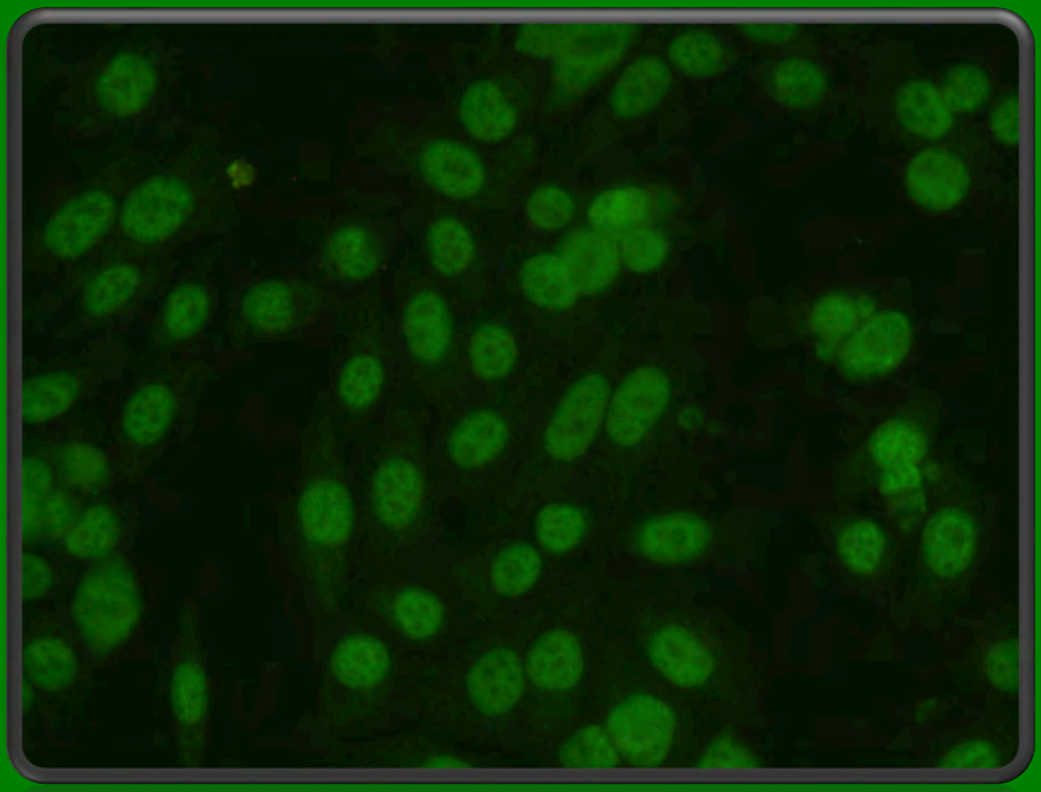


**Organizers**

**Peter Hobson** - *(Peter_Hobson@snp.com.au, Sullivan Nicolaides Pathology, Australia)*
**Gennaro Percannella** - *(pergen@unisa.it, University of Salerno, Italy)*
**Mario Vento** - *(mvento@unisa.it, University of Salerno, Italy)*
**Arnold Wiliem** - *(a.wiliem@uq.edu.au, University of Queensland, Australia)*


http://nerone.diiie.unisa.it/contest-icip-2013/

# COMPETITION ON CELLS CLASSIFICATION BY FLUORESCENT IMAGE ANALYSIS

*Peter Hobson*[1]*, *Gennaro Percannella*[2]*, *Mario Vento*[2]*, *Arnold Wiliem*[3]*

[1]Sullivan Nicolaides Pathology, Australia
[2]University of Salerno, Italy
[3]University of Queensland, Australia

## 1. INTRODUCTION

The Competition on Cells Classification by Fluorescent Image Analysis is hosted by the 20th IEEE International Conference on Image Processing (ICIP), which is the premier forum for the presentation of technological advances and research results in the fields of theoretical, experimental, and applied image and video processing. ICIP is held during September 15-18, 2013 in Melbourne, Australia. This competition is the continuation of the previous event held at International Conference on Pattern Recognition (ICPR) 2012 [1].

### 1.1. Motivation

The contest focuses on the classification of cells extracted from Indirect Immunofluorescence (IIF) images. The IIF is the hallmark protocol for identifying autoimmune diseases such as Systemic Lupus Erythematosus, Sjorgren's syndrome, and Rheumatoid Arthritis [2, 3]. IIF uses the human larynx carcinoma (HEp-2) substrate, which bonds with serum antibodies forming a molecular complex. This complex then reacts with human immunoglobulin conjugated with a fluorochrome and becomes observable at the fluorescence microscope where it reveals the antigen-antibody reaction. Unfortunately, the IIF approach is labour intensive and time consuming [2, 3]. As such, there is a growing interest of using Computer Aided Diagnosis (CAD) systems to overcome such shortcomings.

The interest toward the realization of Computer Aided Diagnosis is witnessed by the growing number of papers proposing algorithms for the analysis of IIF images [4, 5, 6, 7, 8, 9, 10, 11, 12, 13, 14, 15, 16, 17, 18, 19, 20]. Thus, an important issue regards the definition of reliable classification algorithms, and the comparison of their performance on common datasets.

The competition is an international collaboration between the University of Salerno (Italy), the University of Queensland (Australia) and Sullivan Nicolaides Pathology (SNP) - Queensland Medical Testing Laboratory, (Australia). The involvement of the SNP, a relevant laboratory that offers high qualified pathology services for doctors, private hospitals and nursing homes in Queensland northern New South Wales and Darwin, allowed to obtain a significant and valuable dataset that will be used for the contest.

*Indicates equal contribution

### 1.2. Comparison to the previous competition

This collaboration has resulted a significant achievement made by the competition. Compared to the previous competition, the number of data samples are significantly larger: 1,457 images for ICPR2012 [1] versus 68,429 image for ICIP2013. The dataset also introduces two cell patterns less frequent occurring in everyday clinical scenario (i.e. nuclear membrane and golgi). These patterns offer a more realistic evaluation on CAD systems as in clinical scenarios it is needed to make decision upon both frequent occurring and less/rarely occurring cell patterns. Furthermore, having a large dataset enables us to evaluate the systems robustness to within-class and between-class pattern variations.

## 2. CLASSIFICATION TASK

Each participant is given a task to develop a classifier $\varphi$ which classifies a set of HEp-2 cell images. Each image is represented by three-tuple $(\boldsymbol{I}, \boldsymbol{M}, \delta)$ [20] : (1) $\boldsymbol{I}$ represents the cell fluorescence image; (2) $\boldsymbol{M}$ is the cell mask which is automatically extracted and (3) $\delta$ represents the cell positivity strength which has two values weak/borderline or strong. Let $\boldsymbol{Y}$ be a probe image, $\ell$ be its class label and $\mathcal{G} = \{(\boldsymbol{I}, \boldsymbol{M}, \delta)_1, ...(\boldsymbol{I}, \boldsymbol{M}, \delta)_n\}$ be a given gallery set. The classifier's task is to predict the probe label, $\hat{\ell}$. In other words, $\varphi : \boldsymbol{Y} \times \mathcal{G} \mapsto \hat{\ell}$, where ideally $\hat{\ell} = \ell$.

## 3. DATASET

The dataset was obtained between 2011 and 2013 at Sullivan Nicolaides Pathology laboratory, Australia[2]. The dataset contains the following six classes (see Fig. 1 for some examples): [3]

[1]The dataset is available for download at `http://mivia.unisa.it/contest-hep-2/`

[2]We name this dataset as ICIP2013 dataset

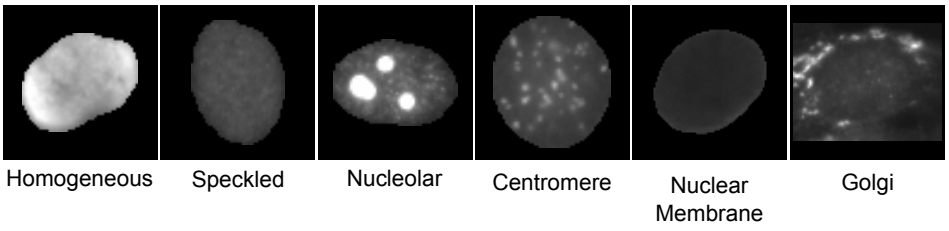


**Fig. 1**. Sample images from ICIP2013 dataset.

- *homogeneous*: a uniform diffuse fluorescence covering the entire nucleoplasm sometimes accentuated in the nuclear periphery;
- *speckled*: these patterns have two sub-categories [3]:
  - *coarse speckled*: densely distributed, variously sized speckles, generally associated with larger speckles, throughout nucleoplasm of interphase cells; nucleoli are negative;
  - *fine speckled*: fine speckled staining in a uniform distribution, sometimes very dense so that an almost homogeneous pattern is attained; nucleoli may be positive or negative;
- *nucleolar*: brightly clustered large granules corresponding to decoration of the fibrillar centers of the nucleoli as well as the coiled bodies;
- *centromere*: rather uniform discrete speckles located throughout the entire nucleus;
- *golgi*: staining of a polar organelle adjacent to and partly surrounding the nucleus, composed of irregular large granules. Nuclei and nucleoli are negative. Diffuse staining of the cytoplasm of dividing cells sometimes with accentuation around chromosomal material;
- *nuclear membrane*: a smooth homogeneous ring-like fluorescence of the nuclear membrane in interphase cells.

The dataset utilises 419 patient positive sera which were prepared on the 18-well slide of HEP-2000 IIF assay from Immuno Concepts N.A. Ltd. with screening dilution 1:80. The specimens were then automatically photographed using a monochrome high dynamic range cooled microscopy camera which was fitted on a microscope with a plan-Apochromat 20x/0.8 objective lens and an LED illumination source. Approximately 100-200 cell images were extracted from each patient serum. In total there were 68,429 cell images extracted. We divided these into 13,596 images for training and 54,833 for testing.

[3]In this dataset, we consider these two sub-categories as one category.

The labeling process involved at least two scientists who read each patient specimen under a microscope. A third expert's opinion was sought to adjudicate any discrepancy between the two opinions. We used each specimen label for the groundtruth of cells extracted from it. Furthermore, all the labels were validated by using secondary tests such as ENA, and anti-ds-DNA to confirm the presence and/absence of specific patterns.

## 4. PARTICIPATION

The competition received more than 100 registrations from around the world with 14 submissions.

In the following we report the members and affiliations of all the teams that participated to the Competition on Cells Classification by Fluorescent Image Analysis. We refer to each method using the name of the corresponding author of the software submission.

**CHANDRAN**: V. Chandran, J. Banks, B. Chen, I. Toro-Reyes *Queensland University of Technology, Australia* .**HAN**: X. Han, J. Wang, Y. Chen, *Ritsumeikan University, Japan* . **KAZANOV**: G.V. Ponomarev, M.S. Gelfand, M.D. Kazanov, *Institute for Information Transmission Problems, Russia* . **MAREE**: R. Marée, *University of Liège, Belgium*. **NANNI**: L. Nanni[1], M. Paci[2,3], J. Hyttinen[2,3], S. Severi[4], [1]*University of Padua, Italy*, [2] *Tampere University of Technology, Finland*, [3] *BioMediTech, Finland*, [4] *University of Bologna, Italy*. **PAISITKRIANGKRAI**: S. Paisitkriangkrai, R. Hill, C. Shen, A. den Hengel, *University of Adelaide, Australia* . **POMPONIU**: V. Pomponiu, H. Hariharan, *University of Pittsburgh, USA*. SARRAFZADEH: O. Sarrafzadeh, H. Rabbani, *Isfahan University of Medical Sciences, Iran* . **SHEN**: L. Shen, J. Lin, S. Yu, *Shenzhen University, China* . **STOKLASA**: R. Stoklasa, *Masaryk University, Czech Republic*. **THEODORAKOPOULOS**: I. Theodorakopoulos, D. Kastaniotis, *University of Patras, Greece*. **THIBAULT**: G. Thibault, *Oregon Health & Science University, USA* .**VESTERGAARD**: A.B.L. Larsen, J.S. Vestergaard, R. Larsen, *Technical University of Denmark, Denmark*. **ZHANG**: L. Liu[1], J. Zhang[2], L. Wang[2], [1]*Australian National University, Australia*, [2] *University of Wollongong, Australia*.

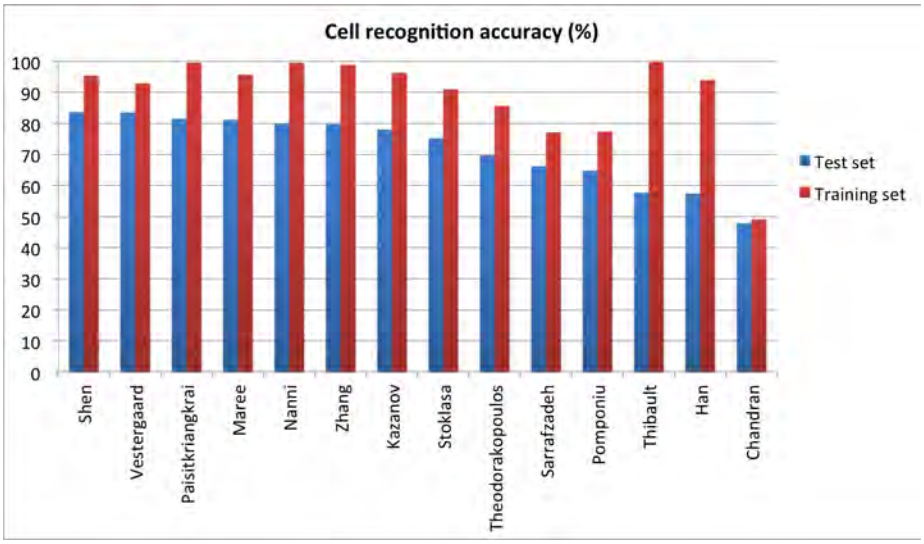


**Fig. 2**. The cell recognition accuracy obtained by the considered methods over the test set.

## 5. EXPERIMENTAL RESULTS

The adopted experimental protocol was the following. Each participant received the training set with the original images of the automatically segmented cells. In particular, for each cell we provided the bounding box and the foreground mask. The cells were provided along with the information about the intensity pattern and the ID of the image they belong to.

The participants used the training set to tune their HEp-2 cells classification system and then they released the executable for the independent evaluation on the test set. It is worth noting that information about the ID of the image the cell belongs to was provided to the participants only for the images of the training set. This information is useful during the tuning phase of the system in order to avoid putting some cells belonging to the same image within both the training and the validation set which could cause to overestimate the real accuracy.

Finally, we ran all the submitted executables on the test set collecting the results that are reported forward. In particular, in Figure 2 we plot the cells recognition accuracy attained by each method on both the training and the test sets, while in Tables 1-14, we report the confusion matrices of all the methods on the test set.

## 6. REFERENCES

[1] P. Foggia, G. Percannella, P. Soda, and M. Vento, "Benchmarking HEp-2 cells classification methods," *Medical Imaging, IEEE Transactions on*, vol. PP, no. 99, pp. 1–1, 2013.

[2] Pier Luigi Meroni and Peter H Schur, "ANA screening: an old test with new recommendations," *Annals of the Rheumatic Diseases*, vol. 69, no. 8, pp. 1420 –1422, 2010.

[3] Allan S. Wiik, Mimi Hier-Madsen, Jan Forslid, Peter Charles, and Jan Meyrowitsch, "Antinuclear antibodies: A contemporary nomenclature using HEp-2 cells," *Journal of Autoimmunity*, vol. 35, pp. 276–290, 2010.

[4] N Bizzaro, R Tozzoli, E Tonutti, A Piazza, F Manoni, A Ghirardello, D Bassetti, D Villalta, M Pradella, and P Rizzotti, "Variability between methods to determine ANA, anti-dsDNA and anti-ENA autoantibodies: a collaborative study with the biomedical industry," *Journal of Immunological Methods*, vol. 219, no. 1-2, pp. 99–107, 1998.

[5] B-N Pham, S. Albarede, A. Guyard, E. Burg, and P. Maisonneuve, "Impact of external quality assessment on antinuclear antibody detection performance," *Lupus*, vol. 14, no. 2, pp. 113–119, 2005.

[6] Petra Perner, Horst Perner, and Bernd Mller, "Mining knowledge for HEp-2 cell image classification," *Artificial Intelligence in Medicine*, vol. 26, pp. 161–173, 2002.

[7] Rico Hiemann, Thomas Bttner, Thorsten Krieger, Dirk Roggenbuck, Ulrich Sack, and Karsten Conrad, "Challenges of automated screening and differentiation of non-organ specific autoantibodies on HEp-2 cells," *Autoimmunity Reviews*, vol. 9, no. 1, pp. 17–22, 2009.

[8] P. Elbischger, S. Geerts, K. Sander, G. Ziervogel-Lukas, and P. Sinah, "Algorithmic framework for HEp-2 fluorescence pattern classification to aid auto-immune diseases diagnosis," in *IEEE International Symposium on*

**Table 1**. Confusion matrix for the CHANDRAN's algorithm.

| % | Centromere | Homogeneous | Nucleolar | Speckled | Nuclear membrane | Golgi |
|---|---|---|---|---|---|---|
| Centromere | **85.99** | 2.54 | 0.48 | 3.44 | 2.63 | 4.93 |
| Homogeneous | 0.72 | **88.30** | 0.53 | 4.04 | 6.13 | 0.28 |
| Nucleolar | 50.32 | 10.23 | **9.49** | 3.97 | 21.46 | 4.54 |
| Speckled | 16.57 | 45.72 | 1.84 | **17.22** | 10.14 | 8.51 |
| NuMem | 19.45 | 24.52 | 3.91 | 1.61 | **49.97** | 0.54 |
| Golgi | 25.58 | 33.18 | 0.53 | 0.00 | 34.20 | **6.51** |

**Table 2**. Confusion matrix for the HAN's algorithm.

| % | Centromere | Homogeneous | Nucleolar | Speckled | Nuclear membrane | Golgi |
|---|---|---|---|---|---|---|
| Centromere | **88.13** | 1.14 | 3.44 | 5.47 | 0.95 | 0.89 |
| Homogeneous | 2.71 | **44.79** | 5.67 | 13.83 | 31.71 | 1.27 |
| Nucleolar | 8.22 | 4.74 | **52.72** | 7.75 | 22.58 | 4.00 |
| Speckled | 20.05 | 15.55 | 3.22 | **51.70** | 8.90 | 0.57 |
| NuMem | 6.03 | 7.98 | 17.99 | 7.71 | **57.36** | 2.93 |
| Golgi | 1.35 | 11.44 | 36.11 | 0.62 | 17.17 | **33.31** |

**Table 3**. Confusion matrix for the KAZANOV's algorithm.

| % | Centromere | Homogeneous | Nucleolar | Speckled | Nuclear membrane | Golgi |
|---|---|---|---|---|---|---|
| Centromere | **93.35** | 0.13 | 2.12 | 3.58 | 0.26 | 0.56 |
| Homogeneous | 0.36 | **68.66** | 5.40 | 10.76 | 12.78 | 2.05 |
| Nucleolar | 1.31 | 1.70 | **88.69** | 2.11 | 3.92 | 2.28 |
| Speckled | 14.84 | 16.22 | 2.57 | **61.24** | 3.81 | 1.33 |
| NuMem | 0.34 | 4.71 | 2.24 | 3.21 | **86.70** | 2.79 |
| Golgi | 0.89 | 9.08 | 10.29 | 3.29 | 22.33 | **54.13** |

**Table 4**. Confusion matrix for the MAREE's algorithm.

| % | Centromere | Homogeneous | Nucleolar | Speckled | Nuclear membrane | Golgi |
|---|---|---|---|---|---|---|
| Centromere | **94.65** | 0.05 | 1.92 | 2.94 | 0.34 | 0.10 |
| Homogeneous | 0.24 | **72.63** | 4.44 | 12.86 | 9.30 | 0.51 |
| Nucleolar | 3.01 | 0.95 | **91.08** | 3.31 | 1.09 | 0.56 |
| Speckled | 20.87 | 10.98 | 3.02 | **61.47** | 3.40 | 0.26 |
| NuMem | 0.11 | 4.51 | 1.16 | 2.39 | **90.95** | 0.89 |
| Golgi | 0.36 | 6.05 | 8.78 | 0.85 | 15.23 | **68.73** |

**Table 5**. Confusion matrix for the NANNI's algorithm.

| % | Centromere | Homogeneous | Nucleolar | Speckled | Nuclear membrane | Golgi |
|---|---|---|---|---|---|---|
| Centromere | **92.59** | 0.17 | 3.43 | 3.08 | 0.23 | 0.50 |
| Homogeneous | 0.67 | **66.29** | 6.04 | 11.14 | 14.44 | 1.42 |
| Nucleolar | 0.86 | 1.82 | **92.45** | 1.41 | 3.03 | 0.42 |
| Speckled | 14.41 | 12.26 | 2.65 | **67.01** | 3.28 | 0.38 |
| NuMem | 0.34 | 2.41 | 2.19 | 1.67 | **89.56** | 3.82 |
| Golgi | 0.56 | 7.43 | 10.59 | 0.66 | 25.95 | **54.82** |

**Table 6**. Confusion matrix for the PAISITKRIANGKRAI's algorithm.

| % | Centromere | Homogeneous | Nucleolar | Speckled | Nuclear membrane | Golgi |
|---|---|---|---|---|---|---|
| Centromere | **92.48** | 0.14 | 2.88 | 3.76 | 0.32 | 0.40 |
| Homogeneous | 0.72 | **70.21** | 7.87 | 11.11 | 9.67 | 0.42 |
| Nucleolar | 1.40 | 0.72 | **92.00** | 2.02 | 3.34 | 0.51 |
| Speckled | 13.01 | 8.92 | 3.54 | **70.84** | 3.36 | 0.33 |
| NuMem | 0.33 | 4.76 | 3.62 | 2.33 | **87.96** | 1.00 |
| Golgi | 1.38 | 2.73 | 13.71 | 3.22 | 12.79 | **66.16** |

**Table 7**. Confusion matrix for the POMPONIU's algorithm.

| % | Centromere | Homogeneous | Nucleolar | Speckled | Nuclear membrane | Golgi |
|---|---|---|---|---|---|---|
| Centromere | **79.88** | 1.19 | 11.67 | 2.68 | 1.15 | 3.42 |
| Homogeneous | 0.10 | **61.95** | 8.88 | 9.84 | 19.04 | 0.20 |
| Nucleolar | 1.38 | 4.85 | **59.09** | 4.02 | 7.21 | 23.45 |
| Speckled | 13.00 | 22.15 | 8.26 | **51.96** | 4.38 | 0.24 |
| NuMem | 0.13 | 3.95 | 11.79 | 0.98 | **78.61** | 4.55 |
| Golgi | 0.26 | 6.35 | 23.38 | 0.23 | 27.23 | **42.55** |

**Table 8**. Confusion matrix for the SARRAFZADEH's algorithm.

| % | Centromere | Homogeneous | Nucleolar | Speckled | Nuclear membrane | Golgi |
|---|---|---|---|---|---|---|
| Centromere | **92.60** | 1.13 | 2.17 | 1.49 | 1.52 | 1.10 |
| Homogeneous | 5.30 | **55.08** | 6.87 | 15.16 | 12.43 | 5.16 |
| Nucleolar | 19.17 | 6.01 | **58.80** | 7.28 | 3.98 | 4.76 |
| Speckled | 26.43 | 18.10 | 3.77 | **46.79** | 4.05 | 0.86 |
| NuMem | 0.62 | 5.77 | 1.07 | 0.98 | **82.99** | 8.58 |
| Golgi | 0.62 | 5.23 | 11.94 | 1.28 | 27.13 | **53.80** |

**Table 9**. Confusion matrix for the SHEN's algorithm.

| % | Centromere | Homogeneous | Nucleolar | Speckled | Nuclear membrane | Golgi |
|---|---|---|---|---|---|---|
| Centromere | **95.13** | 0.40 | 1.63 | 2.00 | 0.46 | 0.38 |
| Homogeneous | 0.39 | **78.15** | 4.92 | 9.14 | 6.64 | 0.76 |
| Nucleolar | 1.13 | 1.70 | **90.31** | 3.36 | 2.33 | 1.18 |
| Speckled | 10.39 | 13.40 | 3.24 | **69.68** | 2.47 | 0.82 |
| NuMem | 0.19 | 4.63 | 1.47 | 1.92 | **90.85** | 0.94 |
| Golgi | 0.89 | 9.67 | 14.76 | 2.40 | 12.23 | **60.05** |

**Table 10**. Confusion matrix for the STOKLASA's algorithm.

| % | Centromere | Homogeneous | Nucleolar | Speckled | Nuclear membrane | Golgi |
|---|---|---|---|---|---|---|
| Centromere | **86.25** | 0.56 | 2.12 | 10.39 | 0.21 | 0.47 |
| Homogeneous | 0.38 | **67.08** | 5.69 | 12.82 | 13.32 | 0.72 |
| Nucleolar | 2.25 | 4.48 | **84.10** | 6.76 | 2.05 | 0.36 |
| Speckled | 14.76 | 13.53 | 3.67 | **64.84** | 2.98 | 0.22 |
| NuMem | 0.31 | 6.71 | 1.86 | 2.65 | **86.77** | 1.69 |
| Golgi | 0.66 | 13.78 | 13.55 | 2.17 | 34.63 | **35.22** |

**Table 11**. Confusion matrix for the THEODORAKOPOULOS's algorithm.

| % | Centromere | Homogeneous | Nucleolar | Speckled | Nuclear membrane | Golgi |
|---|---|---|---|---|---|---|
| Centromere | **90.56** | 0.99 | 2.06 | 5.21 | 0.76 | 0.42 |
| Homogeneous | 0.40 | **64.51** | 1.82 | 10.62 | 21.99 | 0.67 |
| Nucleolar | 10.19 | 1.33 | **76.08** | 3.10 | 3.80 | 5.51 |
| Speckled | 20.62 | 13.24 | 4.77 | **55.94** | 4.86 | 0.57 |
| NuMem | 2.55 | 11.67 | 8.10 | 5.42 | **69.73** | 2.54 |
| Golgi | 8.71 | 1.61 | 19.96 | 1.15 | 25.09 | **43.47** |

**Table 12**. Confusion matrix for the THIBAULT's algorithm.

| % | Centromere | Homogeneous | Nucleolar | Speckled | Nuclear membrane | Golgi |
|---|---|---|---|---|---|---|
| Centromere | **78,98** | 0,05 | 1,2 | 3,81 | 14,1 | 1,86 |
| Homogeneous | 0,12 | **55,56** | 1,59 | 11,83 | 29,55 | 1,34 |
| Nucleolar | 2,73 | 0,65 | **47,31** | 6,22 | 35,99 | 7,11 |
| Speckled | 13,65 | 14,13 | 2,73 | **39,32** | 29,54 | 0,64 |
| NuMem | 0,98 | 5,26 | 5,07 | 5,88 | **81,71** | 1,1 |
| Golgi | 1,09 | 10,52 | 29,46 | 2,73 | 41,76 | **14,44** |

**Table 13**. Confusion matrix for the VESTERGAARD's algorithm.

| % | Centromere | Homogeneous | Nucleolar | Speckled | Nuclear membrane | Golgi |
|---|---|---|---|---|---|---|
| Centromere | **96.21** | 0.25 | 1.34 | 1.44 | 0.46 | 0.30 |
| Homogeneous | 0.30 | **77.34** | 6.11 | 7.15 | 8.46 | 0.63 |
| Nucleolar | 1.17 | 1.68 | **92.76** | 2.31 | 1.09 | 1.00 |
| Speckled | 11.28 | 14.85 | 4.33 | **66.67** | 2.22 | 0.65 |
| NuMem | 0.22 | 2.96 | 1.93 | 2.01 | **92.10** | 0.78 |
| Golgi | 0.39 | 4.47 | 8.39 | 1.97 | 22.53 | **62.25** |

**Table 14**. Confusion matrix for the ZHANG's algorithm.

| % | Centromere | Homogeneous | Nucleolar | Speckled | Nuclear membrane | Golgi |
|---|---|---|---|---|---|---|
| Centromere | **92.37** | 0.56 | 2.70 | 3.87 | 0.36 | 0.14 |
| Homogeneous | 0.53 | **70.26** | 4.93 | 11.70 | 11.70 | 0.89 |
| Nucleolar | 1.60 | 1.58 | **89.28** | 3.57 | 2.88 | 1.09 |
| Speckled | 14.11 | 11.28 | 3.41 | **65.63** | 4.81 | 0.76 |
| NuMem | 0.43 | 7.80 | 1.01 | 2.14 | **87.67** | 0.95 |
| Golgi | 0.92 | 4.93 | 10.10 | 2.24 | 19.04 | **62.78** |


*Biomedical Imaging: From Nano to Macro*, 2009, pp. 562–565.

[9] Tsu-Yi Hsieh, Yi-Chu Huang, Chia-Wei Chung, and Yu-Len Huang, "HEp-2 cell classification in indirect immunofluorescence images," in *Int. Conf. Information, Communications and Signal Processing*, 2009, pp. 1–4.

[10] P. Soda, G. Iannello, and M. Vento, "A multiple expert system for classifying fluorescent intensity in antinuclear autoantibodies analysis," *Pattern Analysis and Applications*, vol. 12, no. 3, pp. 215–226, 2009.

[11] G. Percannella, P. Soda, and M. Vento, "Mitotic HEp-2 cells recognition under class skew," *Lecture Notes in Computer Science (including subseries Lecture Notes in Artificial Intelligence and Lecture Notes in Bioinformatics)*, vol. 6979 LNCS, no. PART 2, pp. 353–362, 2011.

[12] Arnold Wiliem, Peter Hobson, Rodney Minchin, and Brian Lovell, "An automatic image based single dilution method for end point titre quantitation of antinuclear antibodies tests using HEp-2 cells," in *Digital Image Computing: Techniques and Applications*, 2011.

[13] Petter Strandmark, Johannes Ulén, and Fredrik Kahl, "Hep-2 staining pattern classification," in *Int. Conf. Pattern Recognition*, 2012.

[14] Wafa Bel haj ali, Paolo Piro, Dario Giampaglia, Theirry Pourcher, and Michel Barlaud, "Biological cell classification using bio-inspired descriptor in a boosting k-nn framework," in *International Conference on Pattern Recognition (ICPR)*, 2012.

[15] Ilias Theodorakopoulos, Dimitris Kastaniotis, George Economou, and Spiros Fotopoulos, "Hep-2 cells classification via fusion of morphological and textural features," in *IEEE International Conference on Bioinformatics and Bioengineering (BIBE)*, 2012.

[16] Guillaume Thibault and Jesus Angulo, "Efficient statistical/morphological cell texture characterization and classification," in *International Conference on Pattern Recognition (ICPR)*, 2012.

[17] Subarna Ghosh and Vipin Chaudhary, "Feature analysis for automatic classification of hep-2 florescence patterns: Computer-aided diagnosis of auto-immune diseases," in *International Conference on Pattern Recognition (ICPR)*, 2012.

[18] Kuan Li and Jianping Yin, "Multiclass boosting svm using different texture features in hep-2 cell staining pattern classification," in *International Conference on Pattern Recognition (ICPR)*, 2012.

[19] Santa Di Cataldo, Andrea Bottino, Elisa Ficarra, and Enrico Macii, "Applying textural features to the classification of hep-2 cell patterns in iif images," in *International Conference on Pattern Recognition (ICPR)*, 2012.

[20] Violet Snell, William Christmas, and Josef Kittler, "Texture and shape in fluorescence pattern identification for

auto-immune disease diagnosis," in *International Conference on Pattern Recognition (ICPR)*, 2012.

[21] Ilker Ersoy, Filiz Bunyak, Jing Peng, and Kannappan Palaniappan, "Hep-2 cell classification in iif images using shareboost," in *International Conference on Pattern Recognition (ICPR)*, 2012.

[22] Arnold Wiliem, Yongkang Wong, Conrad Sanderson, Peter Hobson, Shaokang Chen, and Brian C. Lovell, "Classification of human epithelial type 2 cell indirect immunofluoresence images via codebook based descriptors," in *IEEE Workshop on Applications of Computer Vision (WACV)*, 2013.

# Table of content

# CELL IMAGE CLASSIFICATION USING HISTOGRAMS, HIGHER ORDER STATISTICS AND ADABOOST

*Vinod Chandran, Jasmine Banks, Wageeh Boles, Brenden Chen, Inmaculada Tomeo-Reyes*

Queensland University of Technology, Brisbane, Queensland, Australia.

**ABSTRACT**

A cell classification algorithm that uses first, second and third order statistics of pixel intensity distributions over pre-defined regions is implemented and evaluated. A cell image is segmented into 6 regions extending from a boundary layer to an inner circle. First, second and third order statistical features are extracted from histograms of pixel intensities in these regions. Third order statistical features used are one-dimensional bispectral invariants [1]. 108 features were considered as candidates for Adaboost [2] based fusion. The best 10 stage fused classifier was selected for each class and a decision tree constructed for the 6-class problem. The classifier is robust, accurate and fast by design.

***Index Terms—*** Cell, Classification, Histogram, Bispectrum, Higher order statistics, Adaboost

## 1. RATIONALE OF THE METHOD

An algorithm for automated cell classification is designed with the following considerations: (a) it must utilize texture information selectively from different parts, (b) it must be robust to rotation and noise, (c) it must capture third order statistical information from pixel intensity producing many features and (d) an optimal fused classifier should be generated for a given problem based on training data. The most original aspect of the methodology is the use of bispectral invariant features [1] from histograms to achieve the desired robustness and accuracy with support from region selection and feature selection using Adaboost [2].

## 2. IMAGE PRE-PROCESSING

It is assumed that individual cell images have been separated and a cell mask image is available. Based on the cell mask, each cell is divided into regions extending from a boundary layer to an inner circle. 6 regions are used in the system described here (listed in Table 1). They are not all disjoint. A histogram of pixel intensities is computed for each region.

## 3. FEATURE EXTRACTION

18 features are extracted from each region – brightness (first order), contrast (second order) and 16 one-dimensional bispectral invariants [1]. These features are designed to be robust to brightness and contrast changes. Histograms of the regions are invariant to rotation of the cell image by design and consequently, the features are as well. Bispectral invariant [1] features are angles and lie in the range between $[-\pi,\pi)$ and the other features are normalized to this range. 108 features were used to train classifiers for each of the HEp-2 cell classes using Adaboost [2]. The number of selected features by their order and the region of the cell they come from are given in table 1.

| Class | Order | | | Region | | | | | |
|---|---|---|---|---|---|---|---|---|---|
| | 1 | 2 | 3 | Outer most | Next outer | Inner disc | Inner ring | Small disc | Inner most |
| HOM | 4 | | 6 | 4 | 3 | 1 | | 1 | 1 |
| CEN | 4 | | 6 | 5 | | 1 | 1 | 1 | 2 |
| NUC | 4 | 1 | 5 | 3 | 3 | 2 | | 2 | |
| SPE | 7 | 2 | 1 | 4 | 2 | 2 | 1 | 1 | |
| NUM | 5 | | 5 | 4 | 4 | 1 | | 1 | |
| GOL | 4 | | 6 | 2 | 2 | 5 | | 1 | |

**Table 1** Number of selected features by order and region

It can be observed that third order statistical features are important for all classes and that the outermost regions close to the cell boundary contain significant discriminative information. The best feature (first stage) was third order for 3 of the classes and first order for the other three.

## 4. CLASSIFICATION

Adaboost [2] is used to generate 10 stage binary classifiers. They are combined in a decision tree. 60% of the ICIP HEp-2 cell classification competition training data were used for training. The best binary classifier was 91% accurate and the overall accuracy for 6 classes was 49.1% on all data. The order of complexity of the algorithm is roughly $O(N^2)+O(RFQ\log_2 Q)$ where $N^2$ is the number of pixels in the cell, $R$ is the number of regions, $F$ is the number of bispectral features and $Q$ is the number of intensity levels. For training $R=6, F=16, Q=256$ and for testing $RF=10$.

## 5. REFERENCES

[1] V. Chandran and S. L. Elgar, "Pattern Recognition using Invariants Defined from Higher Order Spectra – One Dimensional Inputs," *IEEE Trans. Signal Processing*, vol. 41, pp. 205-212, Jan 1993.

[2] Y. Freund and R. E. Schapire, "Experiments with a new boosting algorithm, in 13th Intl. Conf. Artificial Intelligence, 1996.

# FISHER VECTOR OF MICRO TEXTON FOR HEp-2 CELL CLASSIFICATION

Xian-Hua Han, Jian Wang, Yen-Wei Chen

Ritsumeikan University, Japan
{hanxhua@fc, gr0152ie@ed, chen@is}.ritsumei.ac.jp

## 1. RSTIONAL OF THE METHOD

We present a strategy for automatic classification of HEp-2 cell patterns using texture features. As proved in the last year's submissions in the contest of HEp-2 cell classification, the texture features such as local binary pattern (LBP) and its improved version can result in good classification performance. However, LBP only retains the sign (binary) information of the neighbor pixel compared to the focused pixel, and then lead to a lot of information loss, which would greatly reduce classification performance. Therefore, this study explores the distribution of local pixel neighborhoods (called as micro Texton) with a relaxed strategy of parameter Gaussian mixture model instead of a hard quantization, and then appends the gradient with respect to the model parameters for image representation, which also can be called as Fisher vector. The main advantages of the proposed feature representation include: (1) it can include much more information of the local pattern called as micro Texton than the LBP; (2) it represents the local Texton in a parameter Gaussian mixture model (GMM), which would be more accurate than the conventional hard-quantization such as in bag-of feature model; (3) It also appends the gradient of the parameters in (GMM) excluding the distribution of the micro Texton as features. However, we did not consider any spatial information in our proposed features for representing the cell image. In future works, we will combine some spatial information in our strategy. For classifying the cell pattern, we apply random forest classifier which is proved to result in more promising performance than a linear SVM classifier.

## 2. IMAGE PREPROCESSING

In the current version of our strategy, we did not consider noise in HEp-2 cell images, and the original intensity (0~255) is also directly used with any normalization. However, we use the differential vector of a focused pixel to it neighborhoods as our basis pattern, which can partially remove the affect of the absolute intensity variation.

## 3. FEATURE EXTRACTION

This study starts with small pixel neighborhoods of 3×3 local regions and model the statistics of the local differential vector with respect to the center pixel (called micro texton) instead of binary pattern in LBP. Given all possible 3×3 neighborhoods in an image, i.e. $\mathbf{x}^a = [x_c, x_1, x_2, \cdots, x_8]$ where $x_c$ is the intensity of the center pixel and the rest are those of its 8-neighbors. We are intended to investigate the distribution $p(\mathbf{x}^a / I)$ of these vectors in a given image I. In order to remove the effect of the illumination variance, we subtract the intensity of the center pixel from the rest ones and use the difference vector as the micro texton. Then the distribution of the texton can be formulated as $p(\mathbf{x}^a / I) \approx p(\mathbf{x} / I)$, where $\mathbf{x} = [x_1 - x_c, \cdots, x_8 - x_c]$. Assuming the distribution abbeys multiple Gaussian models, we firstly learn the parameters of the multiple Gaussian in the texton space using some training images, and then form a fisher vector characterized by the gradient with respect to the parameters $\lambda$ of the model: $f(\lambda, \mathbf{x}) = \nabla_\lambda \log p(\mathbf{x} / \lambda)$. In our study, the parameters are the means and covariance matrix in the Gaussian mixture model.

## 4. CLASSIFICATION

In our experiments, we use 50 Gaussian models for representing the Texton space appending the gradients of mean and the diagonal elements of covariance matrix for each dimension of the Texton space, and the total feature dimension in the fisher vector is 850. We learn the classification model using random forest classifier with Positive and Intermediate modality. Given any cell and its mask image, the positive or intermediate modality, our system can automatically predict its pattern. With our system and the provided HEp-2 cell data, the evaluated classification rate is about 93% for positive cells, and about 77% for intermediate cells. In addition, the complexity of the proposed system includes two parts: O(KMd) for feature extraction with Gaussian model number K, pixel number M and Texton dimension d, O(LD) with tree number L and feature vector dimension D.

# CLASSIFICATION OF FLUORESCENT CELL IMAGES BASED ON MORPHOLOGICAL PROPERTIES OF STAINED CELL REGIONS

*Gennady V. Ponomarev*[1], *Mikhail S. Gelfand*[1], *Marat D. Kazanov*[1*]

[1]Research and Training Center on Bioinformatics, Institute for Information Transmission Problems, RAS, Russia.

## 1. RATIONALE OF THE METHOD

The main idea of our approach is exploiting for classification the morphological properties of stained cell regions. More specifically, we used for a recognition of the image class the number, size, localization and shape of the stained cell regions. The general scheme of the proposed method is as follows: i) image thresholding using Otsu binarization method [1] along with the construction of normalized version of original image; ii) extraction of image features; iii) image classification using SVM classifier [2].

## 2. IMAGE PREPROCESSING

Our method includes two separate steps of image preprocessing in accordance with two logically distinct groups of extracted image features. The first group of image features were extracted from the binary image obtained from the original one. Thus, the first preprocessing step was the binarization of the image using Otsu method [1]. On the second preprocessing step the normalized image was derived from the original one by a scaling of the image intensity into the interval [0,255].

## 3. FEATURE EXTRACTION

All classes of fluorescent cell images differ by the cell regions or domains that are stained in the image. These domains - nucleoli, nucleus, chromosomes and other cell organells - differ by size, shape, number and localization inside the cell. The main idea of the proposed approach is to segment the stained regions (further referred to as objects) in the image using binarization technique and then to catch as extracted features their morphological properties. Along with the extraction of features from the binary version of image we also gathered several image features using normalized version of the image. Below is the list of extracted features divided into several logical groups:

1) Object number.
2) Object size:
– mean object area;
– maximum object area;
– object area variance.
3) Holes inside objects:
– holes number;
– mean hole area;
– maximum hole area;
– number of big holes.
4) Holes intensity depth:
– mean hole intensity depth;
– maximum hole intensity depth;
– hole intensity depth variance.
5) Foreground/background intensity properties:
– mean foreground intensity;
– foreground intensity variance;
– mean background intensity;
– background intensity variance.
6) Normalized image intensity properties:
– mean image intensity;
– image intensity variance.
7) Object localization:
– mean object-cell boundary distance;
– center-periphery intensity difference.
9) Object shape:
– length of the longest concave arc of object's perimeter;
– convex hull area minus object area.

## 4. CLASSIFICATION

We used the Support Vector Machine (SVM) method [2] for a classification of images using obtained set of image features. The proposed classification method includes two independently trained classification models, which were constructed for positive and intermediate levels of cells image intensity, respectively.

## 5. REFERENCES

[1] N. Otsu, "A threshold selection method from gray-level histograms," *IEEE Transactions on Systems, Man and Cybernetics*, vol. 9, no. 1, pp. 62–66, Jan. 1979.

[2] C. Cortes, V. Vapnik, "Support-vector networks," *Machine Learning*, vol. 20, no. 3, pp. 273–297, 1995.

*Corresponding author: mkazanov@gmail.com

# CLASSIFICATION OF HEP-2 CELLS WITH RANDOMIZED FEATURES

*Raphaël Marée*

GIGA Bioinformatics Core Facility
GIGA-R Bioinformatics and Modeling, Montefiore Institute, University of Liège, Belgium

## 1. METHOD

### 1.1. Overview

We use our generic approach [1] that implies the extraction of random subwindows described by normalized pixel values, the use of extremely randomized trees to generate large sets of visual features, and a final linear SVM classifier using these image signatures. It does not rely on any specific image processing step (denoising, ...). We used parameter values guided by our previous studies and fine-tuned by internal validation on the challenge training set.

### 1.2. Feature generation

Square subwindows are extracted at random positions, using random sizes varying from 50% to 75% of original image sizes as it yields better results on the training set compared to unconstrained sizes used in [2]. Subwindows were then randomly rotated (using right angles and mirroring) to enrich the training set. We limited the total number of extracted subwindows to 550 per image to meet our computational constraints.

Each subwindow was then resized using bilinear interpolation to a fixed-size patch of 16x16 pixels, and encoded in normalized RGB color space.

An ensemble of 50 trees was built using the Extra-Trees algorithm [3]. Each tree was generated using a minimum node sample size equals to 3750 and the default value for the number of evaluated tests at each node. Each node of a tree is a binary test that involves a thresholding on the difference of a pixel and one of its eight direct neighbours. Pixels and thresholds were drawn randomly and at each node the best test among evaluated tests was choosen by the algorithm according to a measure of impurity.

The ensemble of trees is then used to generate an image-level signature inspired by bags of visual words or textons [4, 5]. Instead of using binary encoding as in [4] we considered that each terminal node of a tree is a real-valued feature that corresponds to the number of image subwindows that reach the terminal node divided by the total number of subwindows extracted in the image, similarly to [5].

RM is supported by the GIGA and by the CYTOMINE research project (grant n° 1017072, http://www.cytomine.be), through funding of the Wallonia and the European Regional Development Fund.

### 1.3. Classification

The number of automatically generated features was 243314. A linear SVM was then trained using the training set of 13596 images described by these sparse, high-dimensional, signatures as input of the LIBLINEAR tool [6] using default parameter values (L2-loss SVM (dual) solver, C = 1.0).

Predicting the class of a test image involves similar extraction and description of subwindows, their propagation through trees to generate its signature, and the final prediction by the linear classifier.

### 1.4. Conclusions

On the training set, our approach yielded roughly 80% recognition rate. Our submission should be viewed as a baseline as no specific algorithm was developed and we believe extending parameter ranges could further improve our performances.

## 2. REFERENCES

[1] Raphaël Marée, Pierre Geurts, and Louis Wehenkel, "Towards generic image classification: a extensive empirical study," *Submitted.*, 2013.

[2] R. Marée, P. Geurts, J. Piater, and L. Wehenkel, "Random subwindows for robust image classification," in *Proc. IEEE CVPR*. IEEE, 2005, vol. 1, pp. 34–40.

[3] P. Geurts, D. Ernst, and L. Wehenkel, "Extremely randomized trees," *Machine Learning*, vol. 36, no. 1, pp. 3–42, 2006.

[4] Frank Moosmann, Eric Nowak, and Frederic Jurie, "Randomized clustering forests for image classification," *IEEE Transactions on PAMI*, vol. 30, no. 9, pp. 1632–1646, 2008.

[5] Raphaël Marée, Pierre Geurts, and Louis Wehenkel, "Content-based image retrieval by indexing random subwindows with randomized trees," *IPSJ Transactions on Computer Vision and Applications*, vol. 1, no. 1, pp. 46–57, jan 2009.

[6] R.-E. Fan, K.-W. Chang, C.-J. Hsieh, X.-R. Wang, and C.-J. Lin, "Liblinear: A library for large linear classification," *Journal of Machine Learning Research*, vol. 9, pp. 1871–1874, 2008.

# AUTOMATIC CLASSIFICATION OF HEP-2 INDIRECT IMMUNOFLUORESCENCE IMAGES WITH MULTISCALE AND MORPHOLOGICAL FEATURES

*Loris Nanni[1], Michelangelo Paci[2,3] , Jari Hyttinen[2,3] and Stefano Severi[4]*

[1]University of Padua, [2]Tampere University of Technology, [3]BioMediTech, [4]University of Bologna

## 1. RATIONALE OF THE METHOD

Our system is based on the combination of 3 different descriptors: the multiscale Pyramid Local Binary Pattern (PLBP) [1], Strandmark morphological features (STR) [2] and the canonical Haralick features (HAR) [3]. The 3 feature sets are classified using Support Vector Machines (SVMs) and results are combined according to the sum rule.

## 2. IMAGE PREPROCESSING

Before extracting the 3 feature sets, each image was segmented by using the segmentation masks provided with the HEp-2 training set. Specific preprocessing was performed for the STR feature set and it is reported in the next paragraph.

## 3. FEATURE EXTRACTION

### 3.1 Pyramid Local Binary Pattern

PLBP is based on the Local Binary Pattern (LBP) operator, applied to each of the $l=(0,\ldots,L)$ levels of the gaussian pyramid built from the original image by blurring and downsampling it. We build the gaussian pyramid with a 5 x 5 lowpass kernel and a downsampling ratio $R_x=R_y=2$. The used LBP operator is the uniform rotation invariant LBP with the following neighborhoods: (radius = 1, pixels = 8) and (radius = 2, pixels = 16). *By considering levels 0 (original image), 1 and 2 we get 84 features.*

### 3.2 Strandmark morphological features

STR is a reduced version of the Strandmark features. First the background is removed from the image and the image bins containing less than 0.5% pixels are deleted from the 10 binned image histogram.
The image is then thresholded using 20 equally spaced thresholds from the minimum to the maximum image intensity value. From each of the 20 binary images the following features are computed: (1) number of objects, (2) area, (3) area of the convex Hull, (4) eccentricity, (5) Euler number and (6) perimeter. Then each binary image is used to produce a cut out of the original image. From the 20 cut outs (1) mean intensity and (2) mean entropy are computed. Then (1) mean local standard deviation, (2) mean local entropy and (3) mean local range are computed on the previous cut outs and on new cut outs obtained by replacing the original binary image with an eroded version (erosion kernel 5 x 5 pixels). One more feature set made of (1) mean, (2) median and (3) standard deviation is computed on the magnitude of the gradient of the original image smoothed with 10 diverse σs equally spaced in the interval [0.6, 10.5].
Finally the image aspect ratio is included as the last feature. This feature set is made of 311 features and it is extracted first from the original image thus getting the feature vector F1. The same features are extracted by smoothing the original image by a Gaussian kernel (σ=1 and σ=2.5), thus getting feature vectors F2 and F3. *The final feature vector is the concatenation of F1, F2-F1 and F3-F2 (933 features).*

### 3.3 Harlick features

HAR is used as the third feature set. It is extracted from the grey level occurrence matrices computed with distances 1 and 3 pixels. The used adjacency angles are 0°, 45°, 90° and 135°. *This feature set is made of 104 features.*

## 4. CLASSIFICATION

Classification is performed with radial basis function SVMs, according to the "one versus all" approach. 6 SVMs (one for each class) are trained for each of the 3 feature sets considering the specific class as the positive case (+1) and all the others as negative cases (-1). While testing the system on a test image, each of the 3 feature sets is classified by its corresponding 6 SVMs, the 3 partial score corresponding to the same class are combined by the sum rule in one global score and the greatest among the 6 global scores is considered for assigning the test image to its class.

[1] Qian X et al., "PLBP: An effective local binary patterns texture descriptor with pyramid representation", Pattern Recognition, 44(10–11):2502–15, 2011.

[2] Strandmark P et al., “HEp-2 staining pattern classification”, Pattern Recognition (ICPR), 2012 21st International Conference on, 33–6, 2012.

[3] Haralick R et al., “Textural features for image classification”, IEEE Transactions on Systems, Man, and Cybernetics, SMC-3:610–21, 1973.

# ROBUST HEP-2 CELLS CLASSIFICATION USING MULTI-CLASS BOOSTING WITH HETEROGENEOUS FEATURES

*Sakrapee Paisitkriangkrai, Rhys Hill, Chunhua Shen, Anton van den Hengel*

The Australian Centre for Visual Technologies
The University of Adelaide

## 1. METHOD DESCRIPTION

### 1.1. Raionale of the method

In this paper, we describe an effective and efficient classification framework to automatically recognize different patterns of HEp-2 cells. The basic intuition behind our approach is that, instead of using a single feature to discriminate each class from all other classes, it is better to combine a set of diverse and complementary features. To achieve this objective, we combine several discriminative visual features known to be effective for cell classifications with a robust and scalable multi-class boosting. The advantage of our approach is that it is fast to train, less sensitive to the coice of parameters chosen and has a faster convergence rate than existing multi-class boosting algorithm. We discuss details of our approach in the following sections.

### 1.2. Image preprocessing

**Denoising and normalization** We first apply an image contrast enhancement technique known as histogram equalization. The salt and pepper noise is removed using median filtering in the $3 \times 3$ neighbourhood. For LBP and region covariance, we resize the original image and the mask to the size of $64 \times 64$ pixels.

**Image rotation** To increase the number of training samples and Improve the robustness of the classifier, each cell image is rotated at every $\pi/4$ degrees angle. For each training image, there will be 7 additional images corresponding to $\{\pi/4, \pi/2, \cdots, 7\pi/4\}$ orientations. During testing, a voting scheme is applied as a post-processing step to increase the robustness of decision making. We observe that this simple strategy slightly improves the final classification accuracy.

### 1.3. Feature extraction

**Region covariance** We propose to use the covariance of several image statistics as the visual descriptor [1]. In this paper, we use the following image statistics: the intensity value; the first and second order derivative in the vertical and horizontal directions; and the magnitude of the gradients.

**Local Binary Pattern** Due to the large variation in illumination and shape of cells, we use LBP features to capture the characteristics of cells. LBP describes a local region with the magnitude relations between the centre and neighbouring pixel intensities in the local region. In this paper, we use the extension of LBP, known as CoALBP [2], which can describe complex textures by observing not only each local LBP but also the spatial relations among adjacent LBP.

**Statistical features** We use the statistical data as described in [3]. The features consist of number of objects in the thresholded image; area; area of convex hull; eccentricity; Euler number and perimeter; mean; standard deviation; entropy; range value; constrast; correlation energy; and homogeneity. Interested readers should see [3] for more details.

**Type of Intensities** The type of intensities can be one of the following: positive, negative or intermediate.

### 1.4. Classification

To achieve a high classification accuracy and real-time performance, we employ the multi-class boosting algorithm of [4] that can adaptively select the most discriminative feature in each boosting iteration and combine them into an effective strong classifier. The approach is not only efficient but also effective since it directly maximizes the multi-class margin.

## 2. REFERENCES

[1] O. Tuzel, F. Porikli, and P. Meer, "Region covariance: A fast descriptor for detection and classification," in *Proc. Eur. Conf. Comp. Vis.*, 2006.

[2] R.Nosaka, Y.Ohkawa, and K.Fukui, "Feature extraction based on co-occurrence of adjacent local binary patterns," in *PSIVT*, 2011.

[3] P. Strandmark, J. Ulen, and F. Kahl, "HEp-2 staining pattern classification," in *ICPR*, 2012.

[4] S. Paisitkriangkrai, C. Shen, and A. van den Hengel, "A scalable direct formulation for multi-class boosting," Submitted.

# HEP-2 CELLS CLASSIFICATION USING COMPLETE LOCAL BINARY PATTERNS

*Victor Pomponiu[1] and Harishwaran Hariharan[1]*

Department of Radiology[1], University of Pittsburgh, 15213, PA, USA
{pomponiuv, hariharanh@upmc.edu}

**ABSTRACT**

The classification of the human epithelial cell line (HEp-2) cell images is a clinical important and relatively unexplored area of research. In this paper we present a novel scheme for automatic classification of the staining patterns on single-cell fluorescent images. The approach is based on the Local Binary Patterns (LBP) in order to characterize the textural features of the HEp-2 cell images. After the descriptors are computed, a Nearest Neighbored (NN) is used to perform the classification. The capability of the method is assessed on the ICIP 2013 Cell Classification Contest Training dataset comprising over 13000 cell images pertaining to six cell classes, i.e., Centromere, Golgi, Homogeneous, Nucleolar, NuMem, and Speckled. The result computed with 5 fold cross validation shows 92.2% classification accuracy.

***Index Terms—*** HEp-2 cells, complete local binary patterns (CLBP), bilateral filtering, k-NN classification.

## 1. INTRODUCTION

Indirect immunofluorescence imaging is the technique employed to detect autoantibodies in patient serum, which have been confirmed to be in connection with the occurrence of autoimmune diseases such as systemic autoimmune rheumatic diseases, primary biliary cirrhosis and dermatomyositis. These diseases are detected by a specific fluorescence pattern on a humane epithelial cell line (HEp-2). The fluorescence patterns are in general observed by physicians visually inspecting each slide using a fluorescence microscope. Computer-aided detection (CAD) is used in cell screening as an adjunct procedure to reduce false positives and its efficacy has been observed in many studies.

Finding a good set of features (descriptors) for devising a automatic classification scheme is essential for its success. Several descriptors have been proposed recently in literature: LBP [1] and its variants [2-4], BRIEF [5], BRISK [6], ORB [7] and HOG [8-12].

In this study, we present a technique based on complete LBP (CLPB) that can be used to improve the performance and robustness of CAD schemes. Here, we use the CLBP features to describe the microstructures and textural properties of the following cell patterns: 1) *homogeneous*, with diffuse staining of the interphase nuclei and staining of the chromatin of mitotic cells; 2) *speckled*, characterized by a fine granular nuclear staining of the interphase cell nuclei; 3) nucleolar given by the large coarse speckled staining within the nucleus; 4) *centromere*, with discrete speckles distributed throughout the interphase nuclei; 5) *golgi*, is a type of silver staining, that reveals the morphological traits of the cells, and 6) *numem*.

Once the CLPB features are generated for each cell image, we use Nearest Neighbor (NN) method to classify the image cells, obtained from the ICIP 2013 Cell Classi*f*ication Contest Training dataset [13], into the six patterns.

## 2. PRE-PORCESSING

Firstly, each cell image is binarized and then several properties are extracted, in particular it's bounding box (BB). Further, in order to reduce the size of the feature vector we resized the BB image to a size of $w \times w$ pixels by interpolating the image with interpolation with a Lanczos-2 kernel filter (see Fig. 1).

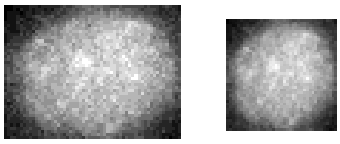

a) b)

**Fig. 1**. a) Illustration of a homogenous cell image; b) its bounding box resized to 40×40 pixels.

Note that, we avoid to apply any filtering, such as median or bilateral filtering since will this operation could eliminate important textural and structural details of the cell image patterns.

## 3. FEATURE EXTRACTION

The features that we employ to classify the image cells is based on CLPB which was proposed by Guo et al. [3] to characterize the local structure in a 3×3 neighborhood.

These features have been successfully applied by the computer vision community for texture classification. Essentially, the CLBP approach is based on the assumption that the local appearance and textural structure can be defined by the histogram of the local sign, magnitude and central pixel defined on a dense grid. The CLBP histograms, of the sign magnitude and central pixel, combine structural and statistical information, and capture the distribution of the classified structures.

The sign LBP feature is obtained as follow: e center pixel is used as a threshold and intensity comparison with the 8 neighboring pixels is performed. Each pixel having intensity value greater than threshold is assigned the binary value 1, otherwise the binary value zero. Afterwards, the 8 binary values are considered as a binary representation of a decimal number, and a histogram of all the corresponding values computed across the image is calculated. In the same manner, are computed the magnitude and the central LBP histograms.

## 4. CLASSIFICATION

The HOG feature extraction algorithm is characterized by the following parameters: the BB image size, the number of samples and the radius size around the central pixel of a neighborhood. Additionally, there are several other parameters related to NN classifier used (i.e., the number of neighbors, the search method and the distance metric). During the training, we optimize these parameters by interactive experimentation: we set all the parameters to their standard values and gradually perturb one parameter at a time, maintaining the result obtained if it improved the average classification accuracy of the algorithm.

The result of this optimization procedure for the entire parameter set was:

- 40×40 pixels for the BB size,
- {1, 2, 3} radii and {8, 16, 24} corresponding samples,
- NN with 7 neighborhoods,
- Exhaustive search,
- Euclidian distance metric.

The feature histograms are used to classify the cells images. To achieve the best classification we used *k*NN classifier with the distance between two cell images a combined histogram dissimilarity between the feature histograms.

## 5. EXPERIMETNAL RESULTS

Classification performance is evaluated by 5 fold cross validation error estimation on the set of 13596 cell images separated into six classes: 2494 homogeneous, speckled 2831, 2598 nucleolar, Centromere 2741, 2208 NuMem and 724 Golgi.

The estimated classification accuracy for the proposed method is 92.2%. The confusion matrix of the CLBP approach method is summarized in Table 1. From the confusion matrix we can notice that the poorest classification accuracy is achieved by Golgi pattern class.

Table 1. Confusion matrix of the proposed method for classification of the cell images. True label is illustrated on the rows while assigned label by the *k*NN classifier is on the columns.

| | **Homogeneous** | **Speckled** | **Nucleolar** | **Centromere** | **NuMem** | **Golgi** |
|---|---|---|---|---|---|---|
| **Homogeneous** | 2362 | 96 | 12 | 4 | 11 | 9 |
| **Speckled** | 109 | 2601 | 57 | 36 | 25 | 3 |
| **Nucleolar** | 30 | 57 | 2438 | 13 | 31 | 29 |
| **Centromere** | 9 | 64 | 41 | 2626 | 1 | 0 |
| **NuMem** | 116 | 33 | 33 | 1 | 2010 | 15 |
| **Golgi** | 34 | 16 | 112 | 15 | 43 | 504 |

## 6. REFERENCES


[1] Z. Guo, L. Zhang, and D. Zhang, "A Completed Modeling of Local Binary Pattern Operator for Texture Classification," *IEEE Transactions on Image Processing*, vol. 19, no. 6, pp. 1657-1663, 2010.

[2] L. Nanni, A. Lumini, and S. Brahnam, "Local binary patterns variants as texture descriptors for medical image analysis," *Artificial Intelligence in Medicine*, vol. 49, no 2, pp. 117-125, 2010.

[3] F. Liu, Z. Tang, and J. Tang, "WLBP: Weber local binary pattern for local image description," *Neurocomputing*, 2013, in press.

[4] B. Fan, F. Wu, and Z. Hu, "Rotationally Invariant Descriptors Using Intensity Order Pooling," *IEEE Transactions on Pattern Analysis and Machine Intelligence*, vol. 34, no. 10, pp. 2031-2045, 2012.

[5] M. Calonder, V. Lepetit, C. Strecha, and P. Fua, "BRIEF: binary robust independent elementary features," in *Proc. of the 11th European conference on Computer vision: Part IV*, 2010, pp. 778-792.

[6] S. Leutenegger, M. Chli, and R.Y. Siegwart, "BRISK: Binary Robust invariant scalable keypoints," in *Proc. Computer Vision*, 2011, pp. 2548-2555.

[7] E. Rublee, V. Rabaud, K. Konolige, and G. Bradski, "ORB: An efficient alternative to SIFT or SURF," in *Proc. Computer Vision*, 2011, pp. 2564-257.

[8] N. Dalal, and B. Triggs, "Histograms of oriented gradients for human detection," in *Proc. Computer Vision and Pattern Recognition*, vol.1, 2005, pp. 886-893.

[9] H. Skibbe, and M. Reisert, "Circular Fourier-HOG features for rotation invariant object detection in biomedical images," in *Proc. International Symposium on Biomedical Imaging*, 2012, pp. 450-453.

[10] Y.S. Salas, D.V. Bermudez, A.M.L. Peña, D.G. Gomez, and T. Gevers, "Improving HOG with image segmentation: application to human detection," In *Proc. 14th International conference on Advanced Concepts for Intelligent Vision Systems*, 2012, 178-189.

[11] J. Zhang, K. Huang, Y. Yu, and T. Tan, "Boosted local structured HOG-LBP for object localization," in *Proc. Computer Vision and Pattern Recognition*, 2011, pp. 1393-1400.

[12] R. Hu, and J Collomosse, "A performance evaluation of gradient field HOG descriptor for sketch based image retrieval," *Computer Vision and Image Understanding*, vol. 117, no. 7, pp. 790-806, 2013.

[13] P. Hobson, G. Percannella, M. Vento, and A. Wiliem, "Competition on cells classication by uorescent image analysis," In: ICIP. (2013), http://nerone.diiie.unisa.it/contest-icip-2013/index.shtml.

# Competition on Cells Classification by Fluorescent Image Analysis

*Omid Sarrafzadeh* [*] *and Hossein Rabbani* [*]

[*] Biomedical Engineering Department, Faculty of advanced medical technology, Isfahan University of Medical Sciences, Isfahan, Iran

## 1. RATIONALE OF THE METHOD

The competition is about the recognition of the staining pattern of the cells obtained by IIF images according to the following classes: Homogeneous, Speckled, Nucleolar, Centromere, Golgi and Nuclear Membrane. The system architecture is as follow: two images are considered as input, original image and related mask image; some preprocessing algorithms are applied on the input image to prepare it for feature extraction step; some texture features are extracted from the prepared image; and finally a model is designed for classification based on mixture models. The proposed system is easy to implement and it takes too little time to run.

## 2. IMAGE PROCESSING

First, the associated input mask is applied to each image to consider information within the mask which is named MaskImage. Then, the contrast of MaskImage is enhanced using histogram equalization. Next, each MaskImage is resized to a 100×100 pixel image using bicubic interpolation method which is named ProImage. This image (ProImage) is ready for feature extraction.

## 3. FEATURE EXTRACTION

Thirty six features are extracted from ProImage as follow: Six statistical features to compute texture measures such as average intensity, average contrast, smoothness, skewness, uniformity and enthropy [1]; seven invariant moments described in [1] which are invariant to translation, scale change, mirroring and rotation; thirteen Haralick features described in [2] and ten discrete wavelet frame texture descriptors described in [3] with three multiresolution levels. So the features matrix is a 36×n matrix in which n denotes the number of samples. The features matrix is then processed by mapping each row's means to 0 and deviations to 1. Then the new features matrix is processed using principal component analysis so that each row is uncorrelated. This uncorrelated features matrix is used for classification.

## 4. CLASSIFICATION

In this stage we have an uncorrelated features matrix with 36×13596 dimensions in which 36 is the number of features for each image and 13596 is the number of samples (images). These samples should be classified into six groups, so there are 6 classes for classification. The number of training sets is 13596. The maximum probability normal classifier is used and the parameters of Gaussian distributions for each class is determined using STPRtool function mlcgmm described by Franc and Hlavac [4]. We made the additional assumption of diagonality of the class covariance matrices to achieve better results. For testing sets the procedure expressed for training sets is repeated and the classification itself is performed by function maxnormalclass described in [5].

## 5. REFERENCES

[1] Rafael C. Gonzalez and Richard E. Woods, *Digital Image Processing*, Prentice Hall, New Jersey, 3rd edition, 2007.

[2] Robert M. Haralick, "Statistical and structural approaches to texture," *Proc. IEEE*, vol. 67, no. 5, pp. 786-804, 1979.

[3] M. Sonka, V. Hlavac and R. Boyle, *Image processing, Analysis, and Machine Vis*ion, Thomson Learning, United States of America, 2008.

[4] V. Franc and V. Hlavac, Statistical pattern recognition toolbox for MATLAB 2004-2011. http://cmp.felk.cvut.cz/cmp/software/stprtool/dwstprtool.html

[5] T. Svoboda, J. Kybic and V. Hlavac, *Image processing, Analysis, and Machine Vis*ion, *A MATLAB companion*, Thomson Learning, United States of America, 2008.

# HEP-2 CELL CLASSIFICATION USING ROTATIONALLY INVARIANT FEATURES

*Linlin Shen, Jiaming Lin and Shiqi Yu*

School of Computer Science & Software Engineering, Shenzhen University, China

## ABSTRACT

Human Epithelial type 2 (HEp-2) cells play an important role in the diagnosis of autoimmune disorder. Traditional approach relies on specialists to observe HEp-2 slides via the fluorescence microscope, which suffers from a number of shortcomings like being subjective and labor intensive. Pattern recognition techniques have been recently introduced to this research issue to make the process automatic.

We propose in this paper a framework using rotationally invariant features, dense SIFT features + bag of words and pairwise Co-occurrence local binary pattern for HEp-2 classification. For SIFT approach, a large number of SIFT features were clustered to form a dictionary, which was then used for cell representation. For pairwise LBP, the uniform pattern LBP operator was applied to two neighboring points for feature extraction. Finally, the two features were fused and input to a SVM (Support Vector Machine) for classification.

***Index Terms***— SIFT, Local Binary Pattern, Support Vector Machine

## 1. Rationale of the method

We developed three systems, namely SIFT, CoLBP and Fusion for the ICIP 2013 contest. For SIFT approach, dense sampling was used to extract a large number of SIFT features, which were then used to learn a dictionary with 1024 words for cell representation. CoLBP use a pair of Co-occurrence LBP operators for feature extraction. Compared to classical LBP, the approach extracts LBP features from two neighborhood points. Fusion approach fuses both SIFT and CoLBP features for cell representation. For all of the three systems, SVM classifier was finally used for classification.

## 2. IMAGE PREPROCESSING

No special image processing method was adopted here, the cell images were directly used for feature extraction and classification.

## 3. FEATURE EXTRACTION

### 3.1. SIFT

Multi-scale, i.e. $20 \times 20$, $36 \times 36$, $40 \times 40$ etc. dense sampling was used for interesting point location. Classical SIFT descriptor was then adopted to extract SIFT histograms at theses interesting points. The extracted SIFT features were then used to learn a dictionary with 1024 words. The dimension of feature for this approach is thus 1024 [1].

### 3.2. CoLBP

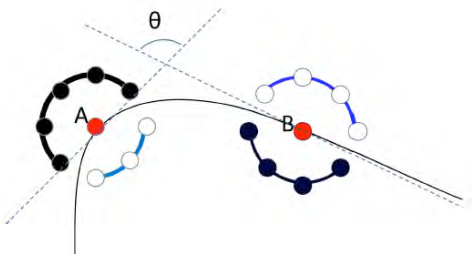


As shown in the figure, the uniform pattern LBP operator was applied to two neighboring points for feature extraction. To make such feature rotationally invariant, the neighboring point B was located at certain distance along the gradient direction of A [2].

### 3.3. Fusion

The two features were finally fused at feature level after normalization.

## 4. CLASSIFICATION

Given the three features, a SVM with linear kernel was finally used to classify the cell image into one of the six classes. Two-fold cross validation was used to tune the parameters.

## REFERENCES

[1] G. Csurka, C. R. Dance, L. Fan, J. Willamowski, and C. Bray, "Visual categorization with bags of keypoints," in *Workshop on Statistical Learning in Computer Vision, ECCV*, 2004, pp. 1-22.

[2] Xianbiao Qi, Rong Xiao, Jun Guo and Lei Zhang. "Pairwise Rotation Invariant Co-occurrence Local Binary Pattern," *Proceedings of ECCV 2012, Lecture Notes in Computer Science*, Vol. 7577, pp. 158-171, 2012.

# HEp-2 Cells Classifier — version v1.4.1

Roman Stoklasa
*Centre for Biomedical Image Analysis, Masaryk University, Brno, Czech Republic*
*xstokla2@fi.muni.cz*

## 1. Overview

Our submitted program is an implementation of a $k$-nearest neighbor classifier build using Metric Similarity Search Implementation Framework (MESSIF). We use global image descriptors such as Local Binary Patterns (LBP), Haralick Features, Color Structure (from the MPEG-7 multimedia descriptors), Granulometry-based descriptor, and statistical texture descriptors. Almost all of them (except for Color Structure) were implemented with help of i3d image processing library developed in our group.

The classification process of each image can be divided into 4 stages: (i) preprocessing, (ii) $k$-NN search, (iii) joining information from all nearest neighbors and inferring of classification estimate and (iv) combination of partial classification estimates and computing final classification.

## 2. Classification process

**i. Preprocessing** The aim of the preprocessing stage is to denoise, normalize and enhance images before image descriptors are used. Denoising is done using the paralel combination of morphological filters. The so-called impulse noise (a small group of pixels with remarkably high intensity) is also removed.

Last step of image preprocessing is contrast enhancement. We estimate the value of ambient illumination by analyzing the background outside the cell, remove this illumination and then apply linear stretch to all intensity values.

**ii. $k$-NN search** Because we use several different image descriptors, we create separate feature space with proper metric for each of them. We use the following descriptors and feature spaces:

- LBP descriptor with the L1 metric
- Haralick Features with the L1 metric
- Color Structure with the L1 metric. This descriptor is computed from a pseudo-color version of grayscale image, where the standard JET color scheme is used.
- Granulometry descriptor, for which we use our own definition of distance function.
- Surface descriptor, which is based on computing cumulative derivative of neighboring pixels. L1 metric is used also in this feature space.
- radial cell structure descriptor with L1 metric

During the $k$-NN search we use custom aggregated distance function which combines different descriptors with different weights. Because we are using $k = 9$, the result of this stage is a list of 9 most similar neighbors to the query image found in the knowledge-base.

**iii. Joining information from neighbors and classification estimate** The input for this stage is a list of $k$ neighboring images obtained in the previous stage. Each image $j$ is associated with the class label $c_j$.

For global descriptors we combine the results of $k$-NN search together with so-called weighted voting — the weight $w_j$ of each found image from the database linearly decays with the distance from the query object. So we compute voting results $p_1, \ldots, p_6$ for each of the 6 classes. These 6 numbers form so-called *classification estimate* $E = (p_1, \ldots, p_6)$, where $i$-th number $p_i$ expresses the preference, that the query image belongs to the $i$-th class.

**iv. Combination of classifications** For each query image we evaluate 3 different $k$-NN searches, so we obtain 3 different classification estimates $\left(E^{(1)}, E^{(2)}, E^{(3)}\right)$ and we need to combine them together. The final preference number $P_i$ for $i$-th class is the sum of $H_i + M_i$, where $H_i$ is a harmonic mean and $M_i$ is a multiplication of the preference numbers $p_i^{(1)}, p_i^{(2)}$ and $p_i^{(3)}$ belonging to the $i$-th class. The classification result is the category $c_i$ with the highest preference number $P_i$.

## 3. Acknowledgement

A big thanks goes to Tomas Majtner and David Svoboda, who helped with the development of previous version of the classifier.

# HEP-2 CELLS CLASSIFICATION USING MULTI-LEVEL THRESHOLDING AND MORPHOLOGICAL FEATURES

*Ilias Theodorakopoulos and Dimitris Kastaniotis*
Electronics Laboratory, Physics Department,
University of Patras, Greece.
{ iltheodorako, dkastaniotis }@upatras.gr

## 1. RATIONALE OF THE METHOD

Staining patterns presented on IIF slides are characterized by great variability. Fluorescence intensity is distributed either in structured, stochastic or intermediate manner. Every fluorescence pattern group is characterized by unique optical properties originating from the nature of the depicted cells.
In order to express appropriately these characteristics as numerical values forming a representative vector, a novel set of morphological features which is a variant of the two dimensional Boolean texture models is incorporated.

## 2. IMAGE PREPROCESSING

On each cell image a median filter is applied in order to eliminate isolated intensity extremities. The original image is then normalized by subtracting the minimum value of the filtered image, and then dividing each pixel's value by the difference between maximum and minimum intensity of the filtered image. The pixel values are then clipped in order to fit in the range between 0 and 1.

## 3. FEATURE EXTRACTION

Subsequently, a set of binary images are constructed via application of thresholding operation to the image, utilizing a set of 14 equally spaced values in the range of [0,1] as threshold values. Significant amount of information is carried by the resulting sequence of binary images regarding the spatial distribution of intensities on the depicted staining pattern, expressed in the form of patterns of homogenous regions of Boolean "True" value, namely objects, with differentiating properties along the various threshold levels. In order to quantify this information, Connected Component Analysis is performed in each binary image, and the following set of morphological features is computed for each of them: Number of detected objects, density in binary image and mean objects' solidity, where objects of size less than 1% of the mean objects' size of each binary image, are considered as noise and ignored during the calculation of the above features. Finally, the complexity of the cell's contour is considered as an additional feature. We chose to quantify the complexity as the difference between the cell's contour and the perimeter of the equivalent circle. Further details on the incorporated features can be found on [1].

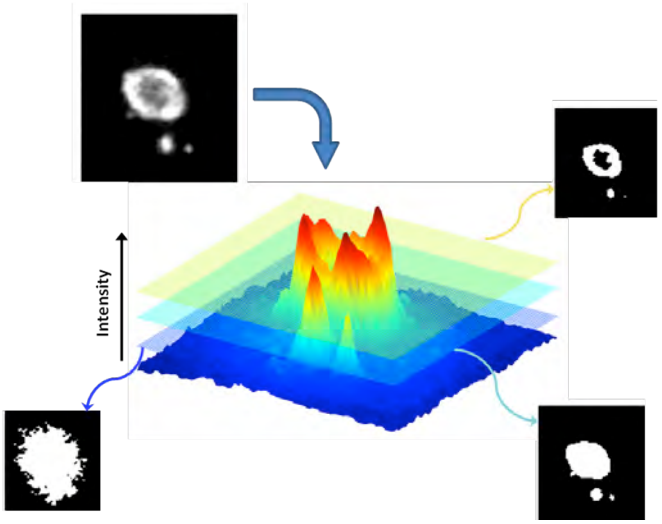


## 4.CLASSIFICATION

The resulting feature vector is normalized by subtracting the mean vector and dividing each feature by the standard deviation of the corresponding values of the training set. Cell images of positive and intermediate intensities are normalized separately, using the corresponding statistics from the training set.

The final classification is performed using the standard k-NN classification rule. Cell images of positive and intermediate intensity are classified separately, using the feature vectors corresponding to training images of the same intensity.

## 11. REFERENCES

[1] Theodorakopoulos, I., Kastaniotis, D., Economou, G., Fotopoulos, S., *HEp-2 Cells classification via fusion of morphological and textural features*, Bioinformatics & Bioengineering (BIBE), 2012 IEEE 12th International Conference on , vol., no., pp.689,694, 11-13 Nov. 2012.

# AUTOMATIC CELL CLASSIFICATION USING STATISTICAL FEATURES

*Guillaume THIBAULT and Izhak SHAFRAN*

Center for Spoken Language Understanding, Oregon Health & Science University, Portland Or, USA

## ABSTRACT

This abstract presents an automatic and efficient cell classification by fluorescent image analysis method, based on using two different families of statistical texture descriptors and a classifier. The method provides a high classification rate for the dataset under study.

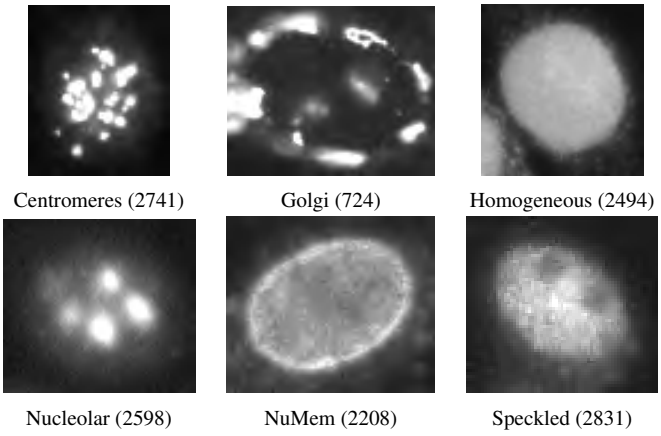


**Fig. 1**. Examples of typical cells for each category (and the number of individual), provided by the ICIP 2013 "Competition on Cells Classification by Fluorescent Image Analysis".

***Index Terms*—** Cell classification, Fuzzy Size Zone Matrix (FSZM), Multiple Local Binary Pattern (MLBP).

## 1. METHOD DESCRIPTION

The image to process are under exposed (histogram on the left), fuzzy and highly noisy (see figure 1). But commons illumination and contrast correction algorithms are particularly sensitive to noise. In order to avoid such tricky and hazardous pre-processing, we use two different statistical descriptors which are not or slightly sensitive to such issues.

First, the Fuzzy Size Zone Matrix (FSZM, not published yet) is a fuzzy version of GLSZM [1], which provides a statistical representation by the estimation of a bivariate conditional probability density function of the image distribution values. Then features are moments of order $-2$ to $2$ computed on such a matrix.

Second, the Multi-resolution Local Binary Patterns (MLBP) [2], is a rotation and gray level invariant technique which attributes to each pixel a unique code according to its neighborhood. Then the histogram of codes (from $0$ to $35$, because of the rotation invariance) characterizes the texture.

This multi-classes problem is decomposed into $6$ binary sub-problems of classification (one per class, in order to simplify the global problem and then improve the results), for each class two classifiers (on per descriptor) are built with Random Forest [3][1] and the probabilities provided by models are averaged in order to provide a final probability for the cell under study to belong to the class. The cell under study is then labelled with the class corresponding to the highest probability. The table 1 shows the results for each sub-problem, which are particularly efficient according to the image to classify.

| | FSZM | MLBP |
|---|---|---|
| Centromeres | 89.32 | 93.15 |
| Golgi | 86.8 | 77.86 |
| Homogeneous | 88.19 | 79.31 |
| Nucleolar | 83.41 | 87.95 |
| NuMem | 88.68 | 91.99 |
| Speckled | 79.84 | 76.77 |

**Table 1**. Predictions (in $\%$) obtained for each sub-problem

## 2. REFERENCES

[1] Guillaume Thibault, Jesus Angulo, and Fernand Meyer, "Advanced statistical matrices for texture characterization: Application to dna chromatin and microtubule network classification," in *IEEE International Conference on Image Processing (ICIP)*, September 2011, pp. 53–56.

[2] Timo Ojala, Matti Pietikainen, and Topi Maenpaa, "Multiresolution gray-scale and rotation invariant texture classification with local binary patterns," *IEEE Transactions on Pattern Analysis and Machine Intelligence*, vol. 24, no. 7, pp. 971–987, July 2002.

[3] Leo Breiman, "Random forests," *Machine Learning*, vol. 45, no. 1, pp. 5–32, 2001.

[1] One of the last advanced techniques in the aggregation of classification trees.

# HEP-2 CELL CLASSIFICATION USING SHAPE INDEX HISTOGRAMS WITH DONUT-LIKE SPATIAL POOLING

*Anders B. L. Larsen, Jacob S. Vestergaard, Rasmus Larsen*

Department of Applied Mathematics and Computer Science
Technical University of Denmark
Kongens Lyngby

## 1. RATIONALE OF THE METHOD

We adopt a standard pipeline for supervised image classification: Preprocessing of images, extraction of meaningful features and finally classification. The parameters involved are tuned using a cross validation scheme. The originality of the method consists primarily of the choice of features, namely a histogram based second order image descriptor encompassing the circular nature of the cells. The main benefit of this pipeline is that it is rich in the explanatory power, while its principle is simple to explain. However, the richness of the extracted features can result in reduced interpretability and increased dimensionality. Thus, a relatively sophisticated – and time consuming – classification algorithm is needed; here we use kernel support vector machines (k-SVMs).

## 2. IMAGE PREPROCESSING

The image preprocessing is very limited. We do two things for preparing each image for feature extraction: First, each image $\mathcal{I}$ is augmented with its logarithmic representation $\log_e \mathcal{I}$. Second, each representation is mapped linearly to $[0, 1]$ such that their minimum attain a value of zero and their maximum a value of one. Thus, the features described below are extracted from both representations of each image.

## 3. FEATURE EXTRACTION

For each image, a feature vector is built consisting of: 1) The 'intensity' of each image (NEGATIVE/INTERMEDIATE/ POSITIVE) as an integer flag, 2) morphological features extracted from the provided mask (including area, eccentricity, major and minor axis length, perimeter), and 3) the donut-like shape index histogram feature (for both image representations).

The most significant feature descriptor consists of weighted histograms, of second-order image features, over a number $K$ of band-shaped regions (donuts). Each region is defined by its distance to the center pixel of the image, i.e., its radius $r_i$. The weight for each pixel is assigned based on a Gaussian distribution centered on the radial band. The weight $w_j$ for the $j$'th pixel with image coordinates $(x_j, y_j)$ to the histogram for the $i$'th donut region is found as $w_j = \exp\{-\frac{\left(\sqrt{x_j^2+y_j^2}-r_i\right)^2}{2\sigma^2}\}$ where the origin $(0, 0)$ is defined as the center of the image and $\sigma$ is the standard deviation of the Gaussian. Thus, features collected in each donut region $\mathcal{R}_i, i = 1, \ldots, K$ describes image characteristics *approximately* at a distance $r_i$ from the image center.

We use this ring-like spatial pooling to collect shape index features in five distances from the image center. In brief, the shape index quantifies second order information in the image from the local Hessian eigenvalues [1]. We collect these features at six different scales, for each of the five donut regions, each binned in sixteen bins. This adds $5 \cdot 6 \cdot 16 = 480$ elements for each image representation to the feature vector, to a total of $p = 977$ per image.

## 4. CLASSIFICATION

For classification we have trained kernel SVMs on the supplied training set. We have chosen, by use of cross validation, to use an RBF kernel with $\gamma = \frac{1}{p}$, penalty parameter $C = 15$ and a one-vs-one scheme for multi-class support. In the ten fold cross validation study, we achieve a misclassification rate of approximately three percent.

The computational complexity of the system during testing is combined from two elements, namely feature extraction and classification. The most expensive operation during feature extraction is a 2D FFT, which is in the order of $\mathcal{O}(N \log N)$, where N is the width of a square image. For classification, the k-SVM is linear in the number of support vectors $m$ and the feature dimensionality $p$, thus in the order of $\mathcal{O}(pm)$.

## 5. REFERENCES

[1] Jan J Koenderink and Andrea J van Doorn, "Surface shape and curvature scales," *Image and vision computing*, vol. 10, no. 8, pp. 557–564, 1992.

# HEp-2 Cell Image Classification with Multiple Local Discriminative Codebooks

Lingqiao Liu,
CECS, Australian National University
lingqiao.liu@cecs.anu.edu.au

Jianjia Zhang, Lei Wang
University of Wollongong, NSW 2522, Australia
jz163@uowmail.edu.au, leiw@uow.edu.au

## 1. Introduction

Our proposed solution for the HEp-2 cell image classification is based a improvement of standard Bag-of-Words (BoW) system. Unlike traditional BoW system in which the descriptor for local patches is empirically selected, our algorithm adopts a deep learning scheme to automatically learn the discriminative descriptors from the raw image pixels. The motivation is that different cells can be distinguished by their unique textures but we dont know what descriptor is most suitable for describing such visual pattern. Hence, we decided to utilize the supervised information provided from the class label to guide the design of patch descriptor. More specifically, we employ partial least square analysis to automatically learn a set of discriminative directions to project the local patches into smaller dimension vectors and utilize these vectors as the discriminative descriptor. One issue of this initial idea is that we only have the class label for each image and patches extracted from one image do not necessarily share the same class label with the image. Actually, the difference between cell categories is only reflected on a small number of patches, many patches are common patches shared by many cell categories. To address this issue, we propose to firstly cluster the image patches into few groups and learn the discriminative descriptor from the patches in each group individually. Then for each group, we follow the standard BoW pipeline to build codebook and create histogram representation based on the learned discriminative descriptor. Hence for each image we will have $N$ (the number of groups) histograms representation. We concatenate them to form the final image representation. In the discriminative descriptor learning step, we still assume the patches from one image sharing the same class label of that image. This assumption, as discussed above, is clearly not appropriate. However, because we pre-cluster the patches into groups, we may hope that common patches and discriminative patches will be separated into different groups. This is based on the assumption that common patches and discriminative patches have different appearance. So for the group with more discriminative patches the generated descriptor, codebook and histogram will be more discriminative because the estimated projection will be less affected by the common patches. Of course, for the group with less discriminative patches, the resulted image representation will be less discriminative. But because we build a histogram separately for each group, we can let the classifier, SVM in our case, to assign different weight for different groups and thus avoid the confusion caused by the inappropriate class label assignment.

### 1.1. System Structure

First, the brightness normalization is performed for the input image and the local patches are extracted from each image on a dense sampling grid. In the training stage, these patches are projected by using PCA and a codebook with N codewords are created from the sampled projection coefficients. This codebook will be used to partition all the local patches into $N$ groups. Then a partial least square analysis is performed in each group to obtain d discriminative projections. The discriminative projections from each group will be used to re-project the image patches to low dimensional vectors in each group. Following the BoW pipeline, a codebook will be built for each group and will be employed to obtain the histogram for each image. Histograms from different groups will then be concatenated together to form the final image representation. A SVM will then be learned as the classifier. In the test stage, the image representation generation process will be repeated but we do not need to partition local patches into N groups. We will simply use the stored N group of projections and codebooks to calculate the histogram representation.

### 1.2. Implementation Details

In our implementation, we densely extract image patches with step size 2 pixels. The patch size is 9x9 pixels. we clustered local patches into 5 groups. More groups were tried but no significant improvement was observed. We use NIPALS algorithm to calculate the partial least square projections and fix the projection dimension to 80. We employ linear SVM with square root preprocessing step applying to histogram count.